Int. J. Heat Mass Transfer. Vol. 23, pp. 1479–1492
© Pergamon Press Ltd. 1980. Printed in Great Britain

0017-9310/80/1101-1479 $02.00/0

HEAT TRANSFER IN POLYMER REACTION MOLDING

LY JAMES LEE* and CHRISTOPHER W. MACOSKO

Department of Chemical Engineering and Materials Science, University of Minnesota,
Minneapolis, Minnesota 55455, U.S.A.

(*Received* 28 *September* 1979 *and in revised form* 31 *March* 1980)

Abstract—A theoretical model is proposed for curing in polymer reaction molding operations like casting, thermoset molding or reaction injection molding (RIM), with mold temperature controlled by fluid circulation over the mold wall. Convection and mass diffusion are neglected. A modified separation-of-variables technique for the heat conduction problem with time-dependent boundary conditions is used to determine an analytical expression for the unsteady mold wall temperature profile. The result is then combined with the non-linear differential equations of heat and mass balance for curing polymers and solved numerically. Quasi-static mold wall temperature is also considered. This greatly simplifies the boundary conditions. The quasi-static assumption is tested for several cases and found applicable to polymer reaction molding. Biot number for heat transfer can be used as a convenient parameter to describe the polymer surface boundary condition.

The model was tested with a fast polymerizing RIM polyurethane in a slab mold instrumented with thermocouples. Various mold wall materials were used. Measurements of temperature profiles in the polymer slab and mold wall compare well to model predictions.

NOMENCLATURE

a,	rate of temperature rise $= dT/dt$;
A,	frequency coefficient of reaction rate;
C_A,	concentration of A functional group;
C_n,	function of time;
C_p,	heat capacity;
d,	half mold thickness;
d_1,	mold wall thickness;
d_2,	thickness of cooling/heating fluid channel;
$\mathcal{D}$,	mass diffusion coefficient;
E_a,	reaction rate activation energy;
h_w,	heat transfer coefficient;
H_R,	heat of reaction;
k,	thermal conductivity;
$\imath$,	mold length;
n,	order of kinetic expression;
q,	heat flux;
$\bar{Q}$,	dimensionless heat removed per unit volume;
R,	gas constant;
R_A,	rate of reaction;
T,	temperature;
$\langle T \rangle$,	average flow temperature;
t,	time;
$\bar{v}_w$,	average water velocity;
x,	flow direction;
y,	radial direction;
α,	heat diffusivity;
ρ,	density;
ϕ,	variable of eigenvalue problem;
λ,	eigenvalue;
η,	viscosity.

Subscripts

0,	initial value;
s,	mold wall;
u,	polymer;
w,	cooling/heating fluid.

Dimensionless terms

$$B = E_a/RT_u;$$

$$B(\xi) = \left(\frac{Bi}{1+Bi}\xi - 1\right)\Bigg/\left(1 + \frac{Bi}{(1+Bi)Bi'}\right);$$

$$\tilde{c} = C_A/C_{A0};$$

$$D = k_s \imath/d_1 d_2 \bar{v}_w \rho_w C_{pw};$$

$$k' = C_{A0}^{n-1} d^2 A e^{-B/\alpha_u};$$

$$p_1 = Bi/(1+Bi);$$

$$p_2 = 1 + \frac{Bi}{(1+Bi)Bi'};$$

$$P_n = \left[\frac{Bi}{1+Bi}(\sin\lambda_n/\lambda_n^2 - \cos\lambda_n/\lambda_n) + (\cos\lambda_n - 1)/\lambda_n\right]\Big/(\tfrac{1}{2} - \sin\lambda_n\cos\lambda_n/2\lambda_n);$$

$$P'_n = \left[\frac{p_1}{p_2}(\sin\lambda_n/\lambda_n^2 - \cos\lambda_n/\lambda_n) + (\cos\lambda_n - 1)/\lambda_n - \sin\lambda_n/Bi' + \frac{p_1\lambda_n}{p_2 Bi'}(\cos\lambda_n/\lambda_n^2 + \sin\lambda_n/\lambda_n - 1/\lambda_n^2)\right]\Big/ [(\lambda_n - \sin\lambda_n\cos\lambda_n)/2\lambda_n + \sin^2\lambda_n/Bi' + \lambda_n^2(\sin\lambda_n\cos\lambda_n/\lambda_n + 1)/2Bi'^2];$$

$$\tilde{t} = \alpha_u t/d^2;$$

$$\Delta\tilde{T}_{ad} = \frac{T_{uad} - T_{u0}}{T_{u0}} = \frac{H_R C_{A0}}{\rho_u C_{pu} T_{u0}};$$

$$\tilde{T}_s = T_s/T_0;$$

---

* Present address: The General Tire & Rubber Company, Research Center, Akron, Ohio, U.S.A.

(Portions of this work have been presented at the A.I.Ch.E. Annual Meeting, New York, November 1977.)

$\tilde{T}_u = T_u/T_{u0}$;
$\tilde{T}_w = T_w/T_0$;
$V = \theta - \left(1 - \frac{Bi}{1+Bi}\xi\right)\theta_u(\tau)$;
$\tilde{x} = s/\iota$;
$\tilde{y} = y/d$;
$\theta = (T_s - T_w)/T_0$;
$\xi = (y-d)/d_1$;
$\tau = \alpha_s t/d_1^2$;
$Bi = \frac{h_w d_1}{k_s}$, Biot number;
$Bi' = \frac{h_u d_1}{k_s}$, Biot number;
$Br = \frac{\eta \bar{v}_w^2}{k\Delta T}$, Brinkman number;
$Fo = \frac{\alpha_s t}{d_1^2}$, Fourier number;
$Nu = \frac{hd_1}{k}$, Nusselt number;
$Pr = \frac{C_p\eta}{k}$, Prandtl number;
$Re = \frac{\bar{v}_w x\rho}{\eta}$, Reynolds number;
$St = \frac{h}{\rho C_p \bar{v}_w}$, Stanton number.

INTRODUCTION

A LARGE number of polymer products involve polymerization in fabricating the final shape. Most of these polymerizations are thermally activated. Examples are: rubber compression and transfer molding, thermoset injection molding, and reinforced polyesters. In these processes, a relatively cold prepolymer mixture is placed into a hot mold and the reaction is energized from the surface. A polymerized state moves to the center by heat conduction with continuing reaction. This requires time for heat transfer in addition to reaction. Another group of materials are mixing activated, for example, polyurethane reaction injection molding, RIM. These involve fast exothermic reaction in which large amounts of heat are generated in a short period of time. High temperatures can cause side reactions, degradation, volatilization, and longer cycle times thus heat must be removed from mold by a cooling system. It is obvious that in most of polymer reaction molding operations sharp temperature gradients will exist inside the mold during reaction and curing. Since the material physical properties, surface quality and also the demolding time are largely dependent on thermal changes in the mold, heat transfer is one of the most important steps in the polymer reaction molding processes.

Problems of nonuniform reaction due to heat transfer and the reaction exotherm are well recognized [1–4]. Some qualitative guidelines for processing are given, but there are few analytical studies. Stonecypher *et al.* [5] included heat of reaction in their model for curing thick sections of solid propellants. Hills [4] reported some transient heat transfer calculations to predict cure development in rubber molding. Engelmaier and Roller [6] used transient heat transfer and a time and temperature dependent viscosity to model thickness change in epoxy electrical laminates. Progelhof and Throne [7] considered non-isothermal curing of unfilled polyesters and epoxies. Each of these studies has dealt only with specific types of processes.

In 1976, Broyer and Macosko [8] proposed a more general theoretical model which could predict the temperature change in the mold with isothermal and adiabatic boundary conditions. In comparing the model with a RIM polyurethane mold temperature distribution [9], they found that the predicted temperature rise of the molded polymer, assuming a constant wall temperature, was lower than the experimental results near the mold wall but reasonably close near the center. The deviation was believed to be due to the non-isothermal response of the mold wall. A more realistic model is needed to explain accurately reaction and curing of polymers in molds, especially in a case of fast highly exothermic reaction molding such as the RIM process. Product properties and the demolding operation can then be pre-controlled. A model is proposed here which considers heat transfer through the molded polymer, the mold wall, and the circulating fluid.

MATHEMATICAL MODEL

A two-dimensional schematic diagram of a mold shape is shown in Fig. 1. The polymerizing liquids are injected between two fairly thick steel or aluminum plates which are cored for water cooling/heating. In Fig. 1 the cores are approximated as a rectangular cavity.

Following is a summary of the assumptions which seem appropriate for the curing stage of a general polymer reaction molding process:

1. No flow.
2. Homogeneous and well-mixed reaction system.
3. One-dimensional heat conduction.
4. Negligible molecular diffusion.

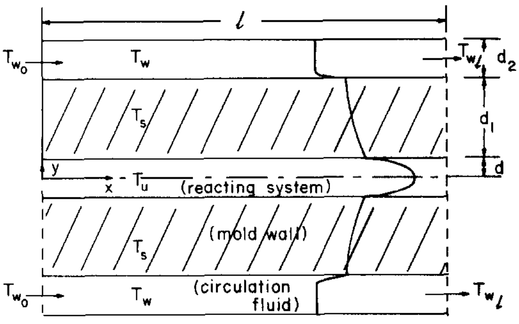

FIG. 1. Two-dimensional schematic diagram of a polymer reaction mold.

5. nth order kinetics.
6. Constant properties α, ρ, C_p of polymer, mold wall and circulation fluid. Heat of reaction H_R is also constant.
7. Turbulent flow of circulation fluid.
8. Intimate contact of surface between the reacting polymer and the mold wall.

In most polymer reaction molding processes, the fill or flow time is significantly less than the total cure time [8] so that flow can be neglected in the system, assumption 1. Good mixing, assumption 2, is a fundamental requirement of a successful operation. For a well mixed reaction system the reactants can be thought of as uniformly distributed in the whole mold and to polymerize from liquid monomers to a solid-like polymer. Only homogeneous reactions are considered here. Some complex systems like foaming and reactions with phase separation (for example, segmented polyurethanes) are not treated. Based on this model, they can be further analyzed.

Most molded parts are thin in one dimension, and the heat transfer can be reduced to a slab calculation, assumption 3. For polymer reactions, the order of magnitude of diffusion is much smaller than the reaction. Thus, it appears reasonable to neglect diffusion of reactants in the mold curing stage.

Determination of kinetics, particularly beyond the gelation, is difficult. For lack of precise data, it seems best to assume an nth order reaction and Arrhenius temperature dependence throughout the entire cure, assumption 5.

Material properties, thermal diffusivity, density and heat capacity of reacting mixture, mold wall, and circulation fluid, are assumed constant to simplify the calculation. This is roughly acceptable, since nearly all thermosetting materials are amorphous. Thus, thermal properties change little with reaction from liquid to solid within the temperature range of a typical cure [10, 11]. However, changes in thermal properties with extent of reaction and temperature can be readily included in our numerical solution. If one type of reaction predominates, then it is also reasonable to assume that heat of reaction, H_R, is constant throughout the reaction.

In practice, the fluid velocity of cooling/heating fluid circulating over the mold wall is usually high, so a turbulent velocity profile can be assumed. This will largely simplify the mathematical model. Intimate contact of surface between the reacting polymer and the mold wall is assumed so that the continuity of temperature at the surface is valid [12].

Thus with these assumptions, the basic equations of this system can be written as

(a) Polymer phase

$$\text{heat transfer } \rho_u C_{pu}\frac{\partial T_u}{\partial t} = \underset{\text{(conduction)}}{k_u\frac{\partial^2 T_u}{\partial y^2}} + \underset{\text{(generation)}}{H_R A\,\mathrm{e}^{-E_a/RT_u}C_A^n}, \tag{1}$$

$$\text{reaction } -\frac{\partial C_A}{\partial t} = A\,\mathrm{e}^{-E_a/RT_u}C_A^n, \tag{2}$$

with initial conditions

$$\left.\begin{aligned} T_u &= T_{u0} \quad (3)\\ C_A &= C_{A0} \quad (4)\end{aligned}\right\} \quad \text{at } t = 0, \text{ for all } 0 \le y \le d,$$

and boundary conditions

$$\frac{\partial T_u}{\partial y} = 0 \qquad \text{at } y = 0, \text{ for } t > 0, \tag{5}$$

$$T_u = T_s \qquad \text{at } y = d, \text{ for } t > 0, \tag{6}$$

or

$$-k_u\frac{\partial T_u}{\partial y} = -k\frac{\partial T_s}{\partial y} \qquad \text{at } y = d, \text{ for } t > 0. \tag{7}$$

(b) Mold wall phase

$$\rho_s C_{ps}\frac{\partial T_s}{\partial t} = k_s\frac{\partial^2 T_s}{\partial y^2}, \tag{8}$$

with initial condition

$$T_s = T_w = T_0 \qquad \text{at } t = 0, \quad \text{for } d \le y \le d + d_1, \tag{9}$$

and boundary conditions are

Equations (6) and (7) plus

$$-k_s\frac{\partial T_s}{\partial y} = h_w(T_s - T_w) \qquad \text{at } y = d + d_1, \quad \text{for } t > 0. \tag{10}$$

(c) Cooling/heating fluid phase

$$d_2\bar{v}_w\rho_w C_{pw}\frac{\partial T_w}{\partial x} = -k_s\left.\frac{\partial T_s}{\partial y}\right|_{y=d+d_1}, \tag{11}$$

with boundary condition

$$T_w = T_0 \qquad \text{at } x = 0. \tag{12}$$

Boundary conditions (6) and (7) are continuity conditions between the two regions.

The heat transfer coefficient h_w in boundary condition (10) is an empirical value [13] which is usually correlated with the Nusselt number $Nu = Nu(Re, Pr, Br, l/d) = hd_1/k$ or the Stanton number $St = St(Nu, Re^{-1}, Pr^{-1}) = h/\rho C_p\bar{v}_w$. A simple expression of heat transfer coefficient correlated from Reynolds analogy and the Taylor–Prandtl modification [14] is used here.

$$h_w = \frac{C_{pw}\rho_w\bar{v}_w}{l}\int_0^l \frac{0.03(Re_x)^{-0.2}}{1 + 2.1(Re_x)^{-0.1}(Pr - 1)}\,\mathrm{d}x \tag{13}$$

where x is the flow direction.

For simplicity, we assume that the heat transfer in the x-direction, the flow direction, is negligible in both the polymer phase and the mold wall phase even though the cooling water temperature is allowed to vary in this direction as indicated in equation (11). Since the cooling water temperature does not change significantly (<5°C) compared to other temperature changes in most actual polymer reaction molding cases, this approximation is thought to be suitable.

Dynamic model for mold wall temperature

The differential equation for heat transfer in the mold wall, equation (8), combined with boundary conditions (6) and (10) can be solved analytically.

Approaches to heat transfer problems of this type were discussed by a number of authors during the early 1960s. Ojalvo [15] adapted a separation of variables approach to solve the transient conduction problem. The technique was basically a quasi-steady solution superimposed on a transient response. The former accounted for external disturbances while the latter were composed of elements which were intrinsic to the system (i.e. eigenvalues). However, Ojalvo did not present a complete solution of the problem. Ölçer [16] applied finite integral transforms to the general solution of three-dimensional transient heat conduction problems with general boundary conditions (including the first, second, and third kind, or mixed type boundary conditions that were functions of space and time). He also used the same method to solve a number of particular heat conduction problems [17–20]. Some other methods for similar heat conduction problems [21–23] are also available in the literature.

To solve our particular problem we have used a modified separation of variables approach and the self-adjoint concept. First, we define dimensionless variables and terms

$$\theta = \frac{T_s - T_w}{T_0}, \quad \xi = \frac{y-d}{d_1}, \quad \tau = \frac{k_s t}{\rho_s C_{ps} d_1^2}, \qquad Bi = \frac{h_w d_1}{k_s}, \quad \theta_u = \frac{T_u - T_w}{T_0}, \tag{14}$$

then equations (8)–(10) and (6) become

$$\frac{\partial \theta}{\partial \tau} = \frac{\partial^2 \theta}{\partial \xi^2} \tag{15}$$

with I. C.

$$\theta(0,\xi) = 0, \qquad \text{for } 0 \le \xi \le 1$$

and B. Cs.

$$\left.\begin{aligned} &\theta(\tau,0) = \theta_u(\tau,0), \\ &\frac{\partial \theta}{\partial \xi}(\tau,1) + Bi\,\theta(\tau,1) = 0. \end{aligned}\right\} \quad \text{for } \tau > 0$$

Second, we define a new variable

$$V(\tau,\xi) = \theta(\tau,\xi) + a(\tau)\theta_u(\tau,0) + b(\tau)\xi. \tag{16}$$

Substituting this new variable V into equation (15), we find that

$$a = -1 \quad \text{and} \quad b = \frac{Bi\,\theta_u(\tau)}{1 + Bi}, \tag{17}$$

and

$$V = \theta - \left(1 - \frac{Bi}{1 + Bi}\xi\right)\theta_u(\tau), \tag{18}$$

such that boundary conditions can be homogenized. Equation (15) then becomes

$$\frac{\partial V}{\partial \tau} = \frac{\partial^2 V}{\partial \xi^2} + \left(\frac{Bi}{1+Bi}\xi - 1\right)\frac{\partial \theta_u(\tau)}{\partial \tau}, \tag{19}$$

with I. C.

$$V(0,\xi) = \left(\frac{Bi}{1+Bi}\xi - 1\right)\theta_u(0),$$

and B. Cs.

$$V(\tau,0) = 0,$$

$$\frac{\partial V}{\partial \xi}(\tau,1) + Bi\,V(\tau,1) = 0.$$

Third, we define a self-adjoint eigenvalue problem with operator:

$$\frac{\partial^2 \phi}{\partial \xi^2} = -\lambda^2 \phi \tag{20}$$

with B. Cs.

$$\phi(0) = 0,$$

$$\frac{\partial \phi}{\partial \xi}(1) + Bi\,\phi(1) = 0.$$

The solution of equation (20) is

$$\phi_n(\xi) = \sin \lambda_n \xi \tag{21}$$

where λ_n is the nth eigenvalue of the characteristic equation:

$$\tan \lambda + \frac{\lambda}{Bi} = 0. \tag{22}$$

Fourth, using separation of variable technique, let

$$V(\tau,\xi) = \sum_{n=1}^{\infty} C_n(\tau)\phi_n(\xi). \tag{23}$$

With the boundary conditions and initial conditions, the problem can be solved. The details are given in Appendix A.

The solution is

$$\begin{aligned} \tilde{T}_s(\tau,\xi) = \sum_{n=1}^{\infty} P_n \Bigg[& \frac{T_{u0}}{T_0}\tilde{T}_u(\tau,0) - \tilde{T}_w(\tau) \\ & - \lambda_n^2 \, \mathrm{e}^{-\lambda_n^2 \tau} \int_0^{\tau} \mathrm{e}^{\lambda_n^2 \tilde{\tau}} \left(\frac{T_{u0}}{T_0}\tilde{T}_u(\tilde{\tau},0) \right. \\ & \left. - \tilde{T}_w(\tilde{\tau}) \right) \mathrm{d}\tilde{\tau} \Bigg] \sin \lambda_n \xi \\ & + \left(1 - \frac{Bi}{1 + Bi}\xi\right)\left(\frac{T_{u0}}{T_0}\tilde{T}_u(\tau,0) \right. \\ & \left. - \tilde{T}_w(\tau)\right) + \tilde{T}_w(\tau) \end{aligned} \tag{24}$$

where

$$\tilde{T}_s = T_s/T_0, \quad \tilde{T}_w = T_w/T_0,$$

and

$$P_n = \left[\frac{Bi}{1+Bi}\left(\frac{\sin\lambda_n}{\lambda^2} - \frac{\cos\lambda_n}{\lambda_n}\right) + \frac{\cos\lambda_n - 1}{\lambda_n}\right] \Big/ \left(\frac{\lambda_n - \sin\lambda_n\cos\lambda_n}{2\lambda_n}\right).$$

This is the analytical expression of the transient mold wall temperature.

The circulation fluid temperature can be written in an integral form,

$$\tilde{T}_w(\tau,\tilde{x}) = -D\int_0^{\tilde{x}} \left.\frac{\partial\tilde{T}_s}{\partial\xi}\right|_{\xi=1} \mathrm{d}x + 1, \tag{25}$$

where

$$D = k_s l/d_1 d_2 \bar{v}_w \rho_w C_{pw}, \qquad \tilde{x} = x/l.$$

$\tilde{T}_w$ can be calculated from equation (25)

$$\begin{aligned}\tilde{T}_w(\tau,\tilde{x}) = -D\int_0^{\tilde{x}}\Bigg\{\sum_{n=1}^{\infty} P_n\Bigg[\frac{T_u}{T_0}(\tau,0,x) - \tilde{T}_w(\tau,x)\\ -\lambda_n^2\,\mathrm{e}^{-\lambda_n^2\tau}\int_0^{\tau}\mathrm{e}^{\lambda_n^2\tilde{\tau}}\Bigg(\frac{T_u}{T_0}(\tilde{\tau},0,x)\\ -\tilde{T}_w(\tilde{\tau},x)\Bigg)\mathrm{d}\tilde{\tau}\Bigg]\lambda_n\cos\lambda_n + \left(\frac{Bi}{1+Bi}\right)\\ \times\left[\tilde{T}_w(\tau,x) - \frac{T_u}{T_0}(\tau,0,x)\right]\Bigg\}\mathrm{d}x.\end{aligned} \tag{26}$$

This is an implicit expression of the cooling/heating fluid temperature.

Defining dimensionless variables

$$\tilde{T}_u = T_u/T_{u0}, \quad \tilde{y} = y/d, \quad \tilde{c} = C_A/C_{A0},$$

the differential equations of the polymer phase then become

$$\frac{\alpha_s d^2}{\alpha_u d_1^2}\frac{\partial\tilde{T}_u}{\partial\tau} = \frac{\partial^2\tilde{T}_u}{\partial\tilde{y}^2} + \Delta\tilde{T}_{ad}k'\tilde{c}^n\exp B\left(1 - \frac{1}{\tilde{T}_u}\right) \tag{27}$$

$$-\frac{\alpha_s d^2}{\alpha_u d_1^2}\frac{\partial\tilde{c}}{\partial\tau} = k'\tilde{c}^n\exp B\left(1 - \frac{1}{\tilde{T}_u}\right) \tag{28}$$

where

$$\Delta\tilde{T}_{ad} = \frac{T_{ad} - T_{u0}}{T_{u0}} = \frac{H_R C_{A0}}{\rho_u C_{pu} T_{u0}},$$

$$B = E_a/RT_{u0}, \qquad k' = \frac{C_{A0}^{n-1}d^2 A\,\mathrm{e}^{-B}}{\alpha_u}$$

with I. Cs.

$$\begin{aligned}\tilde{T}_u(0,\tilde{y},\tilde{x}) &= 1, & & 0 \le \tilde{y} \le 1\\ & & \text{for} & \\ \tilde{c}(0,\tilde{y},\tilde{x}) &= 1, & & 0 \le \tilde{x} \le 1\end{aligned} \tag{29}$$

and B. Cs.

$$\text{(i)}\ \frac{\partial\tilde{T}_u}{\partial\tilde{y}}(\tau,0,\tilde{x}) = 0 \qquad \text{for} \quad 0 \le \tilde{x} \le 1, \tag{30}$$

$$\begin{aligned}\text{(ii)}\ \frac{\partial\tilde{T}_u}{\partial\tilde{y}}(\tau,1,\tilde{x}) = \frac{k_s T_0 d}{k_u T_{u0} d_1}\Bigg\{\sum_{n=1}^{\infty} P_n\Bigg[\frac{T_{u0}}{T_0}\tilde{T}_u(\tau,1,\tilde{x})\\ - \tilde{T}_w(\tau,\tilde{x}) - \lambda_n^2\,\mathrm{e}^{-\lambda_n^2\tau}\int_0^{\tau}\mathrm{e}^{\lambda_n^2\tilde{\tau}}\\ \times\Bigg[\frac{T_{u0}}{T_0}\tilde{T}_u(\tilde{\tau},1,\tilde{x})\\ - \tilde{T}_w(\tau,\tilde{x})\Bigg]\mathrm{d}\tilde{\tau}\Bigg]\lambda_n + \frac{Bi}{1+Bi}\\ \times\left[\tilde{T}_w(\tau,\tilde{x}) - \frac{T_{u0}}{T_0}\tilde{T}_u(\tau,1,\tilde{x})\right]\Bigg\}\end{aligned} \tag{31}$$

coupled with

$$\begin{aligned}\frac{\partial\tilde{T}_w}{\partial\tilde{x}}(\tau,\tilde{x}) = -D\Bigg\{\sum_{n=1}^{\infty} P_n\Bigg[\frac{T_{u0}}{T_0}\tilde{T}_u(\tau,1,\tilde{x}) - \tilde{T}_w(\tau,\tilde{x})\\ - \lambda_n^2\,\mathrm{e}^{-\lambda_n^2\tau}\int_0^{\tau}\Bigg[\frac{T_{u0}}{T_0}\tilde{T}_u(\tilde{\tau},1,\tilde{x})\\ - \tilde{T}_w(\tilde{\tau},\tilde{x})\Bigg]\mathrm{e}^{\lambda_n^2\tilde{\tau}}\mathrm{d}\tilde{\tau}\Bigg]\lambda_n\cos\lambda_n\\ + \frac{Bi}{1+Bi}\left[\tilde{T}_w(\tau,\tilde{x}) - \frac{T_{u0}}{T_0}\tilde{T}_u(\tilde{\tau},1,\tilde{x})\right]\Bigg\}.\end{aligned}$$

In most polymer reaction molding processes, since the velocity of the circulation fluid is very high, fluid temperature is essentially independent of time [24]. Thus, boundary condition (31) can be simplified-to:

$$\begin{aligned}\frac{\partial\tilde{T}_u(\tau,1)}{\partial\tilde{y}} = \frac{k_s T_0 d}{k_u T_{u0} d_1}\Bigg\{\frac{Bi}{1+Bi}\left[1 - \frac{T_{u0}}{T_0}\tilde{T}_u(\tau,1)\right]\\ + \sum_{n=1}^{\infty} P_n\Bigg[\frac{T_{u0}}{T_0}\tilde{T}_u(\tau,1)\\ -\mathrm{e}^{-\lambda_n^2\tau}\Bigg(1 + \frac{T_{u0}}{T_0}\lambda_n^2\int_0^{\tau}\\ \times\mathrm{e}^{\lambda_n^2\tilde{\tau}}\tilde{T}_u(\tilde{\tau},1)\mathrm{d}\tilde{\tau}\Bigg)\Bigg]\lambda_n\Bigg\},\end{aligned} \tag{32}$$

for isothermal circulation fluid.

For polymer reaction molding with flow in the mold, the mold wall temperature can be solved by the same method as indicated in Appendix B.

Quasi-static model for wall temperature

The numerical solution of equations (27)–(32) is complex. If a quasi-static assumption is acceptable, the problem can be simplified considerably and equation (8) becomes

$$\frac{\partial^2 T_s}{\partial y^2} = 0, \tag{33}$$

with B. Cs.

$$T_s = T_u \quad \text{at } y = d,$$

$$-k_s\frac{\partial T_s}{\partial y} = h_w(T_s - T_w) \quad \text{at } y = d + d_1,$$

which can be easily solved to give

$$\tilde{T}_s(\xi) = \frac{Bi}{1+Bi}\left[\tilde{T}_w - \frac{T_{u0}}{T_0}\,\tilde{T}_u(0)\right]\xi + \frac{T_{u0}}{T_0}\,\tilde{T}_u(0). \quad (34)$$

The system is then reduced to a set of simple differential equations:

$$\frac{\partial \tilde{T}_u}{\partial \tilde{t}} = \frac{\partial^2 \tilde{T}_u}{\partial \tilde{y}^2} + \Delta \tilde{T}_{ad} k' \tilde{c}^n \exp B\left(1 - \frac{1}{\tilde{T}_u}\right), \quad (35)$$

$$-\frac{\partial \tilde{c}}{\partial \tilde{t}} = k' \tilde{c}^n \exp B\left(1 - \frac{1}{\tilde{T}_u}\right), \quad (36)$$

with I. Cs.

$$\begin{matrix} \tilde{T}_u(0,\tilde{y},\tilde{x}) = 1, & \text{for} & 0 \le \tilde{y} \le 1 \\ \tilde{c}(0,\tilde{y},\tilde{x}) = 1, & & 0 \le \tilde{x} \le 1 \end{matrix} \quad (37)$$

and B. Cs.

$$\frac{\partial \tilde{T}_u}{\partial \tilde{y}}(\tilde{t},0,\tilde{x}) = 0, \qquad \text{for} \quad 0 \le \tilde{x} \le 1 \quad (38)$$

$$\frac{\partial \tilde{T}_u}{\partial \tilde{y}}(\tilde{t},1,\tilde{x}) = \left(\frac{k_s T_0 d}{k_u T_{u0} d_1}\right)\left(\frac{Bi}{1+Bi}\right) \times \left\{ e^{-\frac{DBi\tilde{x}}{1+Bi}} \left[\frac{DBi}{1+Bi}\,\frac{T_{u0}}{T_0} \int_0^{\tilde{x}} \tilde{T}_u(\tilde{t},1,\tilde{x}') \times e^{\frac{DBi\tilde{x}}{1+Bi}}\, d\tilde{x}' + 1\right] - \frac{T_{u0}}{T_0}\,\tilde{T}_u(\tilde{t},1,\tilde{x})\right\}. \quad (39)$$

Comparison of dynamic and quasi-static models

A comparison of the two models is interesting because the quasi-static model is frequently used in heat transfer problems and other more complex systems, but it is seldom tested. The reason is probably that analytical solutions are usually not available in most of these cases. Ferguson and Finlayson [25] proposed some guidelines for using the quasi-static model for a catalytic converter. The guidelines were obtained by summarizing available literature and were based on ratios of time constants for various heat and mass transfer combinations. They are thought to be appropriate for this study too. Since the analytic transient solution of mold wall temperature is available, further comparison of these two models can be carried out.

The dynamic and quasi-static mold wall temperature can be compared through equations (24) and (34):

$$\tilde{T}_s\big|_{\text{dynamic}} = \tilde{T}_s\big|_{\text{quasi-static}} + \sum_{n=1}^{\infty} \times \left\{ P_n \left[\frac{T_{u0}}{T_0}\,\tilde{T}_u(\tau,0) - \tilde{T}_w(\tau) - \lambda_n^2 e^{-\lambda_n^2 \tau} \int_0^{\tau} e^{\lambda_n^2 \tilde{\tau}} \left(\frac{T_{u0}}{T_0}\,\tilde{T}_u(\tilde{\tau},0) - \tilde{T}_w(\tilde{\tau})\right) d\tilde{\tau}\right] \sin \lambda_n \xi \right\}. \quad (40)$$

The dynamic expression is actually the sum of the quasi-static expression and a transient term. The value of the transient term determines the validity of the quasi-static assumption.

The transient term is controlled by the following four parameters:

(i) Fourier number/Dimensionless time

$$\left(Fo = \frac{\alpha_s t}{d_1^2}\right) \Big/ \left(\frac{k_s t}{\rho_s C_{ps} d_1^2} = \tau.\right)$$

(ii) Biot number, $Bi = \dfrac{h_w d_1}{k_s}$.

(iii) Temperature difference between the two surfaces $T_u(\tau,0) - T_w(\tau)$.

(iv) Thermal history,

$$\int_0^{\tau} e^{\lambda_n^2 \tilde{\tau}} \left(\frac{T_{u0}}{T_0}\,\tilde{T}_u(\tilde{\tau},0) - \tilde{T}_w(\tilde{\tau})\right) d\tilde{\tau}.$$

Eckert and Drake [26] discussed the first three parameters for two simple examples. The thermal history term is actually an accumulated effect of the first three parameters in past time.

For a comparison, we assume a ramp-type surface temperature rise for the reacting polymer. Equation (40) then reduces to

$$\tilde{T}_s\big|_{\text{dynamic}} - \tilde{T}_s\big|_{\text{quasi-static}} = \frac{a d_1^2}{T_0 \alpha_s} \sum_{n=1}^{\infty} \frac{P_n}{\lambda_n^2}\left(1 - e^{-\lambda_n^2 \tau}\right) \sin \lambda_n \xi, \quad (41)$$

with $T_{u0} = T_{s0} = T_0$ and $T_u = T_0 + at$, where a is the slope of the ramp (°C s^{-1}). The curves in Fig. 2 show the rate of temperature change as a function of mold thickness and heat transfer coefficient (i.e. water velocity) for safe use of the quasi-static assumption. In the domain above the curves average deviation between the dynamic model and the quasi-static model is greater than ±1°C. Figure 2 indicates that there is a critical wall thickness, ~ 1 cm, above which the quasi-static model is only valid for relatively slow tempera-

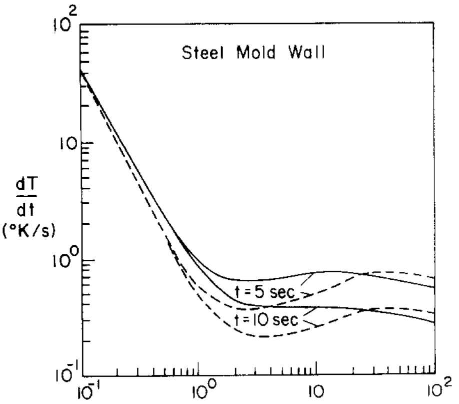

Fig. 2. Average deviation of dynamic behavior from quasi-static behavior. Above the line deviation is greater than ±1°C and use of the full dynamic model may be warranted. Conditions: —— $v_w = 0.5$ m s^{-1} ($h_w = 2.64 \times 10^{-5}$ J m^{-2} s^{-1} K^{-1}); - - - $v_w = 0.1$ m s^{-1} ($h_w = 0.75 \times 10^{-5}$ J m^{-2} s^{-1} K^{-1}).

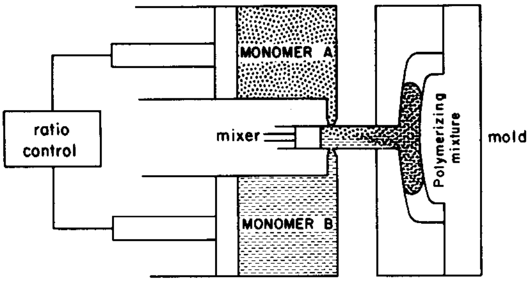

FIG. 3. Schematic diagram of the reaction injection molding process.

ture rise rates. For a slow reaction molding, fabricated in a thin wall mold with good heat conduction properties, the quasi-static model is justifiable. However, some polymer reaction molding operations proceed with a very fast reaction rate in order to make the cycle time shorter. The mold wall is usually much thicker than that used in chemical reactors. A dynamic model will be necessary for a realistic temperature behavior prediction.

Numerical solution of polymer temperature profiles

Equations (27)–(32) and (35)–(39) were solved by the Crank–Nicolson implicit method [27] and the Runge–Kutta method. Twenty equal increments were used in $0 \le \tilde{y} \le 1$. Ten equal increments were used in $0 \le \tilde{x} \le 1$ for the non-isothermal circulation case. The trapezoidal rule and piece-wise integration were used for integration with boundary conditions (39) and (32). Quasilinearization was used to linearize the nonlinear term in equations (27) and (35). This numerical scheme presented no stability problems and gave excellent agreement with analytical solutions.

EXPERIMENTS

RIM

The heat transfer model proposed above was applied to a newly developed polymer processing technique, reaction injection molding or RIM. Instead of fabricating polymeric articles by melt forming of thermoplastic materials, this technology has been developed for rapid *in situ* polymerization to form the desired products directly from monomeric liquids. A brief description of the actual physical conditions of the RIM process is shown in Fig. 3. Two (or more) reactants are metered in the exact stoichiometric ratio and impinge at relatively high velocity in a cylindrical mixing chamber. The mixture flows through the runner and fills the mold in about 2 or 3 s. It reacts rapidly in the mold and solidifies quickly. Parts can be ejected in 30 s and a center exotherm of over 100°C has been measured [9].

Materials

The materials used in this experiment were, A_3, a polyester triol with average molecular weight 2000 (Union Carbide, PCP-0300); B_2, a 4,4′-diphenylmethane diisocyanate derivative with molecular weight 252 (Upjohn, 143L) and dibutyltin dilaurate (M&T Chemical Co., T-12) as a catalyst. These materials were used as received at equal stoichiometry with about 0.1 wt.% catalyst. The triol was heated to ~ 60°C to reduce the viscosity to 0.2 Pa s. The diisocyanate was kept at room temperature. Both materials were degassed under vacuum for at least 2 h to remove water and air dissolved in the reactants, which can cause side reactions and foaming during polymerization. A laboratory scale RIM machine described elsewhere was used to mix the materials and fill in the mold [28].

Adiabatic measurement

A very useful method to derive kinetic data for fast reacting systems is the adiabatic reaction [9, 29, 30]. The temperature rise during an adiabatic reaction provides sufficient kinetic information for the molding calculation. For the change of temperature with time in an adiabatic system, the heat balance equation is

$$\rho_u C_{pu} \frac{\partial T_u}{\partial t} = H_R A\, e^{-E_a/RT_u} C_A^n. \qquad (42)$$

If we assume ρ_u and C_{pu} constant, the extent of reaction will be directly proportional to the heat generated.

$$\frac{C_A}{C_{A0}} = \tilde{c} = \left(\frac{T_{ad} - T_u}{T_{ad} - T_{u0}}\right). \qquad (43)$$

Substituting equation (43) into equation (42), a linear form can be derived

$$\ln \frac{\partial T_u}{\partial t} = \ln F - E_a/RT_u + n \ln\left(\frac{T_{ad} - T_u}{\Delta T_{ad}}\right) \qquad (44)$$

where $F = AC_{A0}^{n-1} \Delta T_{ad}$ and $\Delta T_{ad} = T_{ad} - T_{u0}$.

The variables $\partial T_u/\partial t$, $1/T_u$, and $[(T_{ad} - T_u)/\Delta T_{ad}]$ can be evaluated from the temperature vs time curve of the adiabatic polymerization. By using a multiple linear regression procedure [27] one can obtain the order of reaction n, the activation energy E_a and the frequency coefficient of reaction rate A.

Since the thermal conductivity of polymer is extremely low [10] even a disposable coffee cup can serve as a suitable adiabatic reactor. A fast responding Al–Cr thermocouple wire (gauge 30, time constant ~1 s) was forced through the cup wall with the junction tip seated at the center of the cup and was used to detect the adiabatic temperature rise. It was found that heat loss through the coffee cup during the reaction was negligible. After the center temperature reached the maximum (~180°C), it cooled down very slowly (0.2°C min^{-1} for 150 cm^3 of material). The repeatability was within ±2% of total rise.

Typical adiabatic temperature rise curves are shown in Fig. 4. Circles are the numerical fit by the multiple linear regression procedure. Kinetic parameters can be correlated by either fixing the order of reaction n or with variable n. The results are summarized in Table 1. The values of A and E_a were found to be quite sensitive to the change in n. With the same materials but slightly different catalyst concentration used, reaction order

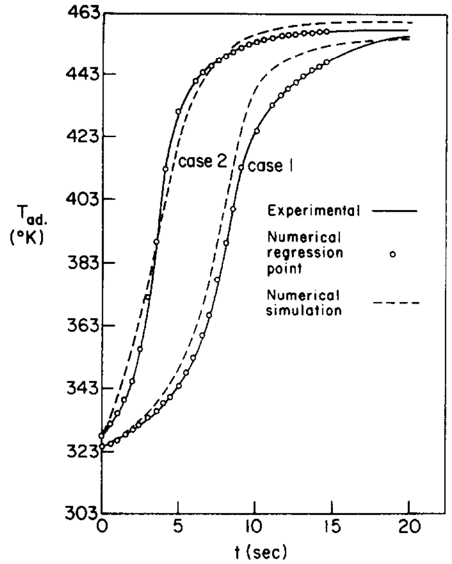

FIG. 4. Two adiabatic temperature rises for thermoset RIM polyurethane reaction, parameters are shown in Table 1.

varied from 1.4 to 3.1. It was also found that the numerical fitting with different number and time space of the data gave different kinetic parameters. This may be an indication that a different kinetic mechanism existed before and after the gel point. There are also some other possible reasons for this: (1) thermal properties ρ, C_p are not constant in the whole cure; (2) the temperature rise is too sharp to make the regression accurate. Thus, mechanistic interpretations of these parameters are not recommended but they are useful for heat transfer analysis. Dashed curves in Fig. 4 are the numerical simulations of adiabatic temperature rises based on the kinetic parameters obtained by the linear regression. There is only slight difference between fixed n and variable n parameters. The fitting is not very good but acceptable for modelling the heat transfer.

Temperature profiles

Experiments were carried out on the laboratory scale RIM machine. An instrumental slab mold with variable thickness and wall materials was constructed. Figure 5 shows the schematic diagram of the in-

Table 1. Results from adiabatic experiments and numerical regression, same material and catalyst concentration used in each case

Case	1		2		3		4		5	
T_{u0}(°C)	51.5		55.0		53.0		57.0		49.0	
ΔT_{ad}(°C)	133.5		130.5		135.0		131.0		135.0	
n(reaction order)	2.0	3.1	2.0	1.4	2.0	1.8	2.0	1.9	2.0	1.5
A(appr. unit)	43.4	33.6	68.2	33.9	56.4	53.9	25.0	21.9	74.0	45.3
E_a(KJ mol^{-1})	41.7	66.4	40.0	25.5	41.6	37.7	37.8	34.0	40.7	28.5

Table 2. Thermal and kinetic data for the experimental RIM process

	Polymer*	Al wall†	Steel wall†	PMMA wall‡	Circulation† water
ρ(kg/m^3 × 10^{-3})	1.14	2.7	8.0	1.17	0.985
C_p(J kg^{-1} K^{-1})	1674.7	896.0	464.7	1373.3	4186.8
k(J m^{-1} s^{-1} K^{-1})	0.15	209.3	49.8	0.19	—
α(m^2 s^{-1})	7.9×10^{-8}	8.65×10^{-5}	1.34×10^{-5}	1.16×10^{-7}	—
Pr	—	—	—	—	3.02
h_w(J cm^{-2} s^{-1} K^{-1})	—	—	—	—	0.0732 ~ 0.264
ΔT_{ad}(K)	~ 133	—	—	—	—
C_{A0}(mol cm^{-3})	0.0036	—	—	—	—
n	2.0	—	—	—	—
E_a(kJ mol^{-1})	~ 40	—	—	—	—
A(appr. unit)	25 ~ 70	—	—	—	—
η(Pa · s)	—	—	—	—	1.0×10^{-5}
d(cm)	0.635	0.8	2.54	1.27	1.27
T_0(K)	313 ~ 333	343 ~ 293	343 ~ 293	343 ~ 293	343 ~ 293
l	18	18	18	18	18
$\tilde{v}_w$(cm s^{-1})	—	—	—	—	16

* From Lipshitz (1976).
† From Eckert and Drake (1972).
‡ From van Krevelan (1972).

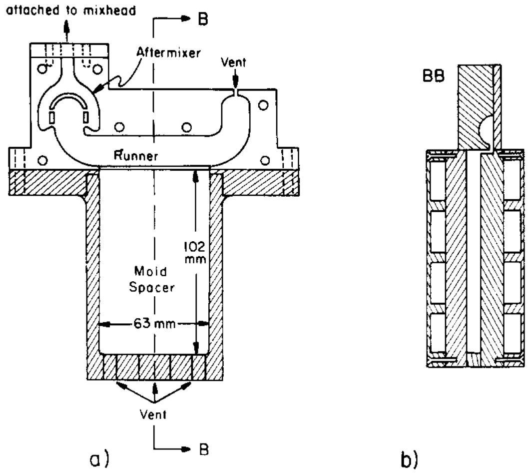

FIG. 5. Schematic diagram of the instrumented mold. (a) Top view of mold spacer and runner system. (b) Side view of mold assembly.

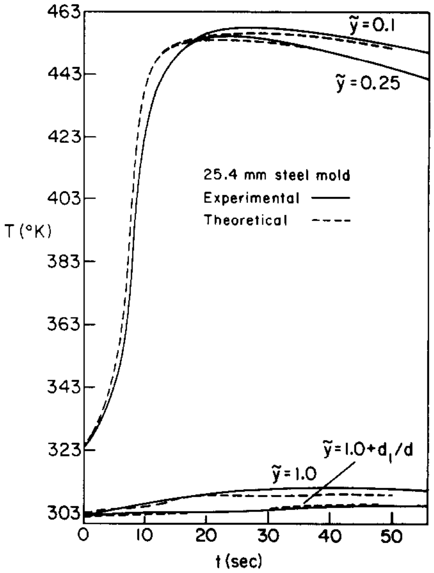

FIG. 6. Comparison of theoretical and experimental temperature profiles for a cold thick steel mold.

strumented mold. Water is circulated through a polymethylmethacrylate, PMMA cavity which covered the top of the mold wall. A mold spacer is sandwiched between the mold walls. An after-mixer connected to the runner and film gate was used to improve the mixing quality, slow down the velocity of mixture and fill the mold without cavitation. Three different mold walls: 25.4 mm steel mold wall with water circulation; 8 mm aluminum mold wall with water circulation and 12.7 mm PMMA mold without water circulation were used. Mold spacers were all 12.7 mm thick aluminum.

Four Al–Cr thermocouple wires, 0.25 mm dia. (30 gauge), were used to record temperature at four positions in the mold: the center of the polymer slab, about half way between the center and surface, and on both sides of the mold wall. The exact location of each thermocouple bead inside the polymer was measured by cutting the part after completion of the experiments. Temperature vs time at each position was recorded with a GOULD 110 strip chart recorder. System response was estimated at 150°C s^{-1}.

Thermal and kinetic data for the reaction system, mold walls and circulation water are summarized in Table 2. For steel and aluminum molds, the circulation water temperature was set both lower and higher than the initial mixture temperature, T_{u0}. For the PMMA mold, wall temperature was kept at room temperature during filling. For modelling the PMMA mold, the outside mold wall surface temperature was assumed to be changed only by free convection and radiation to the adjacent air. These terms are extremely small when the temperature difference between the wall and air is small [14]. Due to the low heat conductivity of the plastic mold, the outside wall surface temperature was almost unchanged during curing.

Figures 6–9 show the measured temperature profiles as function of time. Dashed lines are the numerical simulation from our heat transfer model. The temperature profiles on both sides of 8 mm thick aluminum mold showed no difference on the chart record. Numerical simulation also indicated that this temperature difference was less than 0.5°C so only one wall temperature profile is shown in Fig. 8. However for the plastic mold, Fig. 9, as expected there is a very large difference between inside and outside wall temperature. Figure 10 shows the calculated temperature profiles inside the mold and the plastic wall. The thermocouple bead diameter is 0.05–0.1 cm. For the sharp temperature gradient near the inside plastic wall, the thermocouple bead may measure only an average temperature for part of the wall. Calculated wall temperature profiles at several positions are presented in Fig. 9.

Considering the uncertainty in the physical property measurements and the many assumptions of the

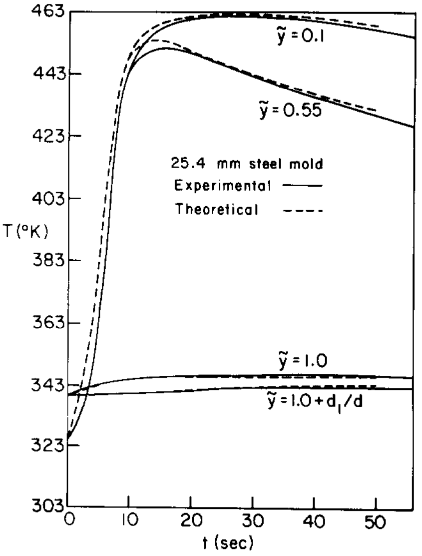

FIG. 7. Comparison of theoretical and experimental temperature profiles for a hot thick steel mold.

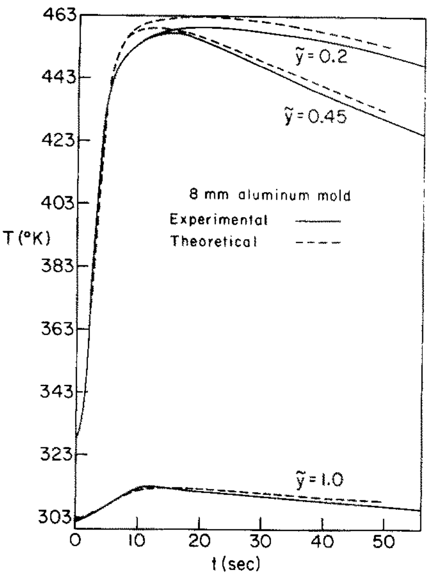

FIG. 8. Comparison of theoretical and experimental temperature profiles for a cold thin aluminum mold.

model, the agreement between experiment and theory is quite good.

Comparison of idealized and non-isothermal cases

With the same reaction system, Fig. 11 shows the temperature profiles at the surface of the molded part under different boundary conditions. The idealized boundary conditions (adiabatic and isothermal) are actually the two extremes. Realistic temperature profiles are between these two extremes and depend on the cooling/heating fluid velocity. Even increasing the cooling fluid velocity to 50 cm s^{-1} does not yield an isothermal mold wall.

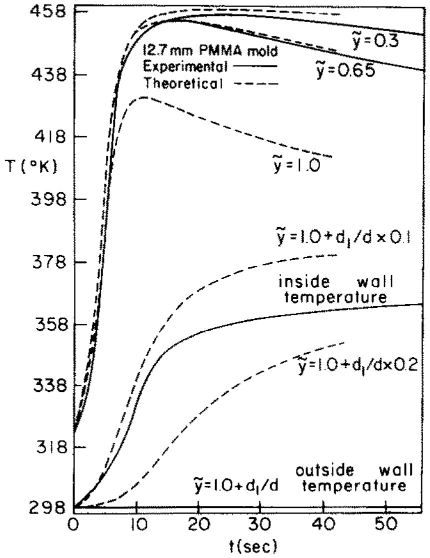

FIG. 9. Comparison of theoretical and experimental temperature profiles for a 12.7 mm thick PMMA mold.

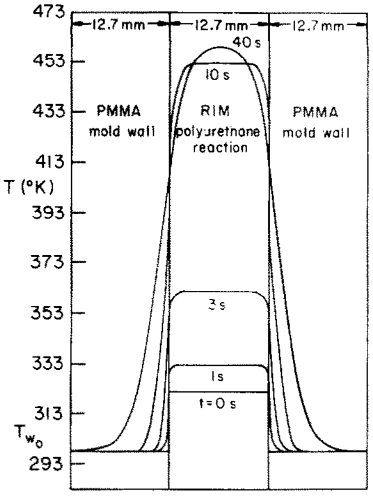

FIG. 10. Calculated temperature profiles inside a PMMA mold.

Figure 12 shows that the temperature changes in the transverse direction, are dramatic. It shows how the temperature is expected to build up in the 3.2 mm thick slab with 3.2 mm heated steel walls. First, the polymer near the wall rises in temperature due to heat conduction from the hot wall. But the heat of polymerization quickly begins to dominate and at about 4 s the centerline temperature is the high point. The gel time of this urethane system is approximately 5 s.

It is found that the Biot number controls the thermal behavior with different boundary conditions. In the quasi-static model, if the water fluid is isothermal, the tangent lines of temperature profiles at the mold wall will coincide at the same pivot point which is on the $T_w = T_0$ line. In isothermal cases this pivot point is on the mold wall. When water velocity decreases (i.e. lower Biot number), the pivot point shifts away from the wall. The distance the pivot point shifts can be

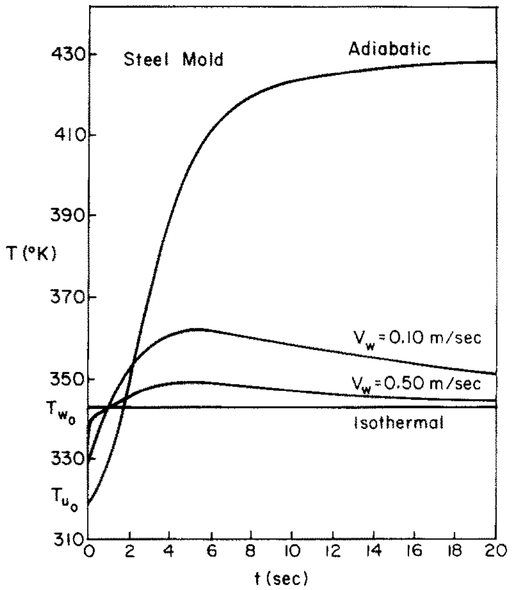

FIG. 11. Comparison of wall temperature, $\tilde{y} = 1$, vs time for various boundary conditions at the mold surface, mold wall $d_1 = 3.2$ mm, polymer $2d = 3$ mm.

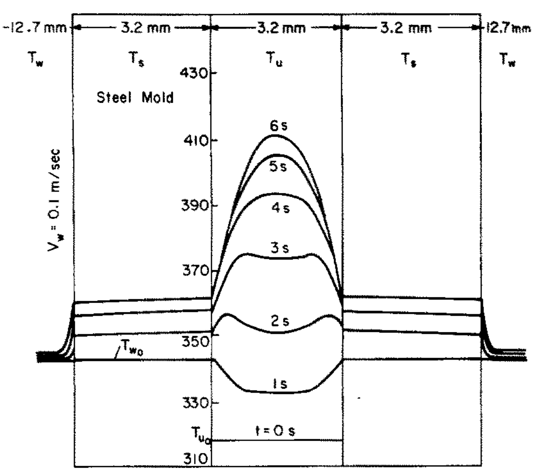

FIG. 12. Temperature profile in a steel mold for a non-isothermal mold wall temperature. The maximum temperature is 413 K at 7 s.

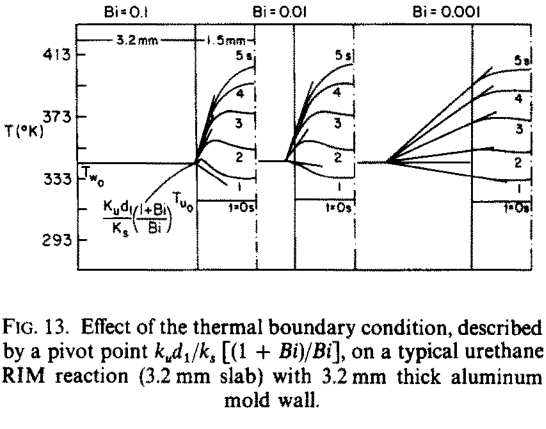

FIG. 13. Effect of the thermal boundary condition, described by a pivot point $k_u d_1/k_s$ $[(1 + Bi)/Bi]$, on a typical urethane RIM reaction (3.2 mm slab) with 3.2 mm thick aluminum mold wall.

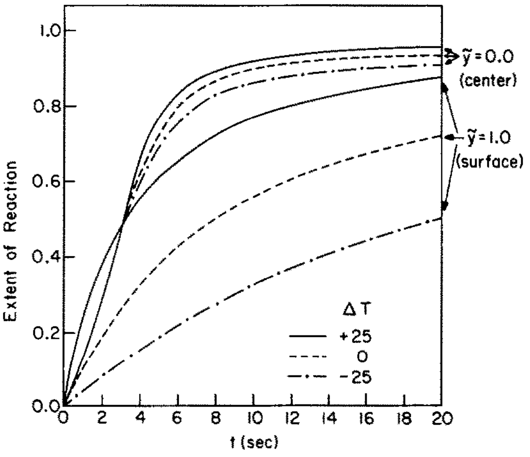

FIG. 14. Comparison of concentration profiles with different mold temperatures. $\Delta T = T_{w_0} - T_{u_0}$; steel mold 3.2 mm thick; 3.2 mm thick polymer.

calculated by a dimensionless parameter, $k_u d_1/k_s$ $[(1+Bi)/Bi]$. The adiabatic condition can be thought as the case where the pivot point moves to infinity. This behavior is shown in Fig. 13. Winter [31] mentioned a similar phenomenon in the viscous dissipation of molten polymer under shear flow.

DISCUSSION

Both the curing model and the experiments show that in a RIM process, the temperature near the mold center is not influenced significantly at short times by the boundary conditions. But of course near the mold wall, temperature profiles are significantly altered. The reacting polymer at the mold center behaves adiabatically due to the fast reaction and extremely low heat conductivity of the polymer. In the adiabatic case, temperature profiles and concentration profiles are always uniform which mean that the reaction is uniform through the whole process. On the other hand, in isothermal and water cooled systems, sharp temperature and concentration gradients near the mold wall occur. These phenomena tell us that in polymer reaction molding, heat transfer is probably a serious problem because the sharp temperature and concentration gradients in those non-adiabatic cases may reduce the physical strength and the surface quality of product.

One way to reduce temperature gradients in the part is to heat the mold. The effect of wall temperature on extent of reaction is illustrated in Fig. 14. Note that if the mold wall is heated 25°C above entering temperature of the reactants there is little effect on the centerline conversion but significant reduction in the difference between center and wall. Thus with a heated mold property development will be much more uniform and will permit faster demolding. However, for highly exothermic reactions, high temperature may cause side reactions, degradation and volatilization. The optimal mold design and molding conditions will depend on the complete understanding of reaction kinetics, thermal behavior, mold quality and economic requirements.

Acknowledgements—The authors would like to thank Dr. Sheng-Tai Lee for his valuable suggestions and discussions in mathematical modeling. This research was supported by grants from the National Science Foundation, Division of Materials Research, Grant No. DMR 75-04508 and the Union Carbide Corporation.

REFERENCES

1. M. B. Horn, *Acrylic Resins*, pp. 38–40 Reinhold, New York (1960).
2. H. Lee and K. Neville, *Handbook of Epoxy Resins*, pp. 77–79 McGraw-Hill, New York (1967).
3. E. N. Doyle, *The Development and Use of Polyester Products*, pp. 297–299 McGraw-Hill, New York (1969).
4. D. A. Hills, *Heat Transfer and Vulcanization of Rubber*, ch. 5, Elsevier, London (1971).
5. T. E. Stonecypher, E. L. Allen, D. E. Mastin and D. A. Willoughby, Special problems in curing highly exothermic propellants, *Chem. Engng Prog. Symp. Ser.* **62**, 7 (1966).

6. W. Engelmaier and M. B. Roller, Temperature-viscosity-time profiles provide some understanding of MLB lamination, *Insulation/Circuits* **21,** No. 4, 43 (1975).
7. R. C. Progelhof and J. L. Throne, Non-isothermal curing of reactive plastics, *Polymer Engng Sci.* **15** (9), 690 (1975).
8. E. B. Broyer and C. W. Macosko, Heat transfer and curing in polymer reaction molding, *A.I.Ch.E. Jl* **22,** 268 (1976).
9. E. B. Broyer, C. W. Macosko, F. E. Critchfield and L. F. Lawler, Curing and heat transfer in polyurethane reaction molding, *Polymer Engng Sci.* **18** (5), 382 (1978).
10. D. W. Van Krevelan, *Properties of Polymers*, ch. 4, 5A and 14, Elsevier, Amsterdam (1972).
11. J. Brandrup and E. H. Immergut, *Polymer Handbook*, pp. V7–12, Wiley, New York (1975).
12. H. S. Carslaw and J. C. Jaeger, *Conduction of Heat in Solids*, Oxford, 2nd edn (1959).
13. R. B. Bird, W. E. Stewart and E. L. Lightfoot, *Transport Phenomena*, Wiley, New York (1960).
14. J. M. Coulson and J. F. Richardson, *Chemical Engineering*, ch. 9, McGraw-Hill, New York (1969).
15. I. U. Ojalvo, Conduction with time-dependent heat sources and boundary conditions, *Int. J. Heat Mass Transfer* **5,** 1105 (1962).
16. N. Y. Ölçer, On the theory of conductive heat transfer in finite regions, *Int. J. Heat Mass Transfer* **7,** 307 (1963).
17. N. Y. Ölçer, On the theory of conductive heat transfer in finite regions with B.C.'s of the second kind, *Int. J. Heat Mass Transfer* **8,** 529 (1965).
18. N. Y. Ölçer, General solutions to a class of heat flow problems in a finite circular cylinder, *Br. J. Appl. Phys.* **18,** 89 (1967).
19. N. Y. Ölçer and J. E. Sunderland, Unsteady heat conduction in finite hollow circular cylinders under time-dependent boundary conditions of the second kind, *Nucl. Engng Des.* **8,** 201 (1968).
20. N. Y. Ölçer, Unsteady temperature distribution in a sphere subjected to time-dependent surface heat flux and internal heat source, *J. Heat Transfer* **91,** 45 (1969).
21. J. Reitzel, Use of boundary sources in problems of heat conduction, *J. Appl. Phys.*, **38,** 3808 (1967).
22. S. S. Filmonov and Y. P. Dvin, Temperature calculation in a multilayered wall acted on by a thermal pulse, *Heat Transfer, Soviet Rev.* **4** (5), 104 (1972).
23. G. Hetsoni, *et al.*, Heat conduction in reactor fuel elements, *Nucl. Sci. Engng* **37,** 329 (1969).
24. L. F. Lawler, Private communication, Union Carbide Co., S. Charleston, W. Virginia (1977).
25. N. B. Ferguson and B. A. Finlayson, Transient modeling of a catalytic converter to reduce nitric oxide in automobile exhaust, *A.I.Ch.E. Jl.* **20,** 539 (1974).
26. E. R. G. Eckert and R. M. Drake, *Analysis of Heat and Mass Transfer*, ch. 4, McGraw-Hill, New York (1972).
27. B. Carnahan, H. A. Luther and J. D. Wilkes, *Applied Numerical Methods*, p. 451, Wiley, New York (1969).
28. L. J. Lee and C. W. Macosko, Design and characterization of a small reaction injection molding machine, *Soc. Plast. Engng Tech. Papers* **24,** 151 (1978).
29. S. D. Lipshitz and C. W. Macosko, Kinetics and energetics of a fast polyurethane cure, *J. Appl. Polym. Sci.* **21,** 2028 (1978).
30. E. B. Richter and C. W. Macosko, Kinetics of fast (RIM) urethane polymerization, *Polym. Engng Sci.* **18,** 1012 (1978).
31. H. H. Winter, Viscous dissipation in shear flows of molten polymers, *Adv. Heat Transfer* **13,** 205 (1977).

APPENDIX A. DERIVATION OF THE ANALYTICAL EXPRESSION OF TRANSIENT MOLD WALL TEMPERATURE

Equation (23) is

$$V(\tau,\xi) = \sum_{n=1}^{\infty} C_n(\tau)\phi_n(\xi) \qquad \text{(A-1)}$$

where

$$C_n(\tau) = \int_0^1 \phi_n(\xi)V(\tau,\xi)\mathrm{d}\xi \Big/ \int_0^1 \phi_n^2(\xi)\mathrm{d}\xi.$$

If we take the dot product of $\phi_n(\xi)$ and equation (19) and integrate it, divide by $\int_0^1 \phi_n^2(\xi)\mathrm{d}\xi$, we obtain

$$\frac{\left\{\dfrac{\partial}{\partial\tau}\displaystyle\int_0^1 \phi_n(\xi)V(\tau,\xi)\mathrm{d}\xi = \int_0^1 \phi_n(\xi)\frac{\partial^2 V}{\partial\xi^2}(\tau,\xi)\mathrm{d}\xi + \dfrac{\partial\theta_n(\tau)}{\partial\tau}\displaystyle\int_0^1 \phi_n(\xi)\left(\frac{Bi}{1+Bi}\xi-1\right)\mathrm{d}\xi\right\}}{\displaystyle\int_0^1 \phi_n^2(\xi)\mathrm{d}\xi} \qquad \text{(A-2)}$$

It can be rewritten and integrated as

$$\frac{\partial C_n(\tau)}{\partial\tau} = \int_0^1 \phi_n\frac{\partial^2 V}{\partial\xi^2}(\tau,\xi)\mathrm{d}\xi \Big/ \int_0^1 \phi_n^2(\xi)\mathrm{d}\xi + \frac{\partial\theta_n(\tau)}{\partial\tau}P_n \qquad \text{(A-3)}$$

where

$$\begin{aligned} P_n &= \int_0^1 \phi_n(\xi)\left(\frac{Bi}{1+Bi}\xi-1\right)\mathrm{d}\xi \Big/ \int_0^1 \phi_n^2(\xi)\mathrm{d}\xi \\ &= \left[\frac{Bi}{1+Bi}(\sin\lambda_n/\lambda_n^2 - \cos\lambda_n/\lambda_n) \right.\\ &\qquad \left. + (\cos\lambda_n - 1)/\lambda_n)\right] \Big/ \left(\frac{\lambda_n - \sin\lambda_n\cos\lambda_n}{2\lambda_n}\right). \end{aligned}$$

The first term on the RHS of equation (A-3) can be integrated by parts and simplified by substitution of boundary conditions. We get

$$\begin{aligned} &\frac{\displaystyle\int_0^1 \phi_n(\xi)\frac{\partial^2 V}{\partial\xi^2}(\tau,\xi)\mathrm{d}\xi}{\displaystyle\int_0^1 \phi_n^2(\xi)\mathrm{d}\xi} \\ &= \left[\phi_n(1)\frac{\partial V}{\partial\xi}(\tau,1) - \frac{\partial\phi_n}{\partial\xi}(1)V(\tau,1)\right. \\ &\qquad \left. + \int_0^1 \frac{\partial^2\phi_n}{\partial\xi^2}(\xi)V(\tau,\xi)\mathrm{d}\xi\right] \Big/ \int_0^1 \phi_n^2(\xi)\mathrm{d}\xi \\ &= \left[\phi_n(1)(-BiV(\tau,1)) - \frac{\partial\phi_n}{\partial\xi}(1)V(\tau,1)\right] \Big/ \\ &\qquad \int_0^1 \phi_n^2(\xi)\mathrm{d}\xi + (-\lambda_n^2 C_n(\tau)) \\ &= -\lambda_n^2 C_n(\tau). \end{aligned} \qquad \text{(A-4)}$$

Equation (A-3) then becomes

$$\frac{\partial C_n(\tau)}{\partial\tau} + \lambda_n^2 C_n(\tau) = P_n\frac{\partial\theta_u(\tau)}{\partial\tau}. \qquad \text{(A-5)}$$

The solution is

$$C_n(\tau) = \mathrm{e}^{-\lambda_n^2\tau}\left[\int_0^\tau \mathrm{e}^{\lambda_n^2\tilde{\tau}}P_n\frac{\partial\theta_u(\tilde{\tau})}{\partial\tilde{\tau}}\mathrm{d}\tilde{\tau} + C\right], \qquad \text{(A-6)}$$

i.e.

$$V(\tau,\xi) = \sum_{n=1}^{\infty} \mathrm{e}^{-\lambda_n^2\tau}\left[\int_0^\tau \mathrm{e}^{\lambda_n^2\tilde{\tau}}P_n\frac{\partial\theta_u(\tilde{\tau})}{\partial\tilde{\tau}}\mathrm{d}\tilde{\tau} + C\right]\sin\lambda_n\xi. \qquad \text{(A-7)}$$

Substituting of initial conditions into equation (A-7), we get

$$V(0,\xi) = \left(\frac{Bi}{1+Bi}\xi - 1\right)\theta_u(0) = \sum_{n=1}^{\infty} C\sin\lambda_n\xi. \qquad \text{(A-8)}$$

If we take the dot product of $\phi_m(\xi)$ and equation (A-8), then integrate it, since $\int_0^1 \phi_m \phi_n \, d\xi = 0$ for $m \neq n$ (orthogonality of eigenfunctions), we get

$$C = P_m \theta_u(0) \qquad \text{(A-9)}$$

and

$$C_n(\tau) = e^{-\lambda_n^2 \tau} P_n \left[\theta_u(0) + \int_0^\tau e^{\lambda_n^2 \tilde{\tau}} \frac{\partial \theta_u(\tilde{\tau})}{\partial \tilde{\tau}} d\tilde{\tau} \right]. \qquad \text{(A-10)}$$

Substituting equations (A-10) and (21) into equation (A-1), the solution is

$$V(\tau, \xi) = \sum_{n=1}^{\infty} e^{-\lambda_n^2 \tau} P_n \left[\theta_u(0) + \int_0^\tau e^{\lambda_n^2 \tilde{\tau}} \frac{\partial \theta_u(\tilde{\tau})}{\partial \tilde{\tau}} d\tilde{\tau} \right] \sin \lambda_n \xi. \qquad \text{(A-11)}$$

Substituting equation (A-11) into equation (18), we get

$$\theta(\tau, \xi) = \sum_{n=1}^{\infty} e^{-\lambda_n^2 \tau} P_n \left[\theta_u(0) + \int_0^\tau e^{\lambda_{\lambda_n}^2 \tilde{\tau}} \frac{\partial \theta_u(\tilde{\tau})}{\partial \tilde{\tau}} d\tilde{\tau} \right] \times \sin \lambda_n \xi + \left(1 - \frac{Bi}{1+Bi} \xi \right) \theta_u(\tau). \qquad \text{(A-12)}$$

If we use dimensionless mold wall temperature $\tilde{T}_w = T_w/T_0$, $\tilde{T}_s = T_s/T_0$, and integrate by parts the integration term, equation (28) becomes

$$\tilde{T}_s(\tau, \xi) = \sum_{n=1}^{\infty} P_n \left[\frac{T_u}{T_0}(\tau, 0) - \tilde{T}_w(\tau) - \lambda_n^2 e^{-\lambda_n^2 \tau} \int_0^\tau \times e^{\lambda_n^2 \tilde{\tau}} \left(\frac{T_u}{T_0}(\tilde{\tau}, 0) - \tilde{T}_w(\tilde{\tau}) \right) d\tilde{\tau} \right] \sin \lambda_n \xi + \left(1 - \frac{Bi}{1+Bi} \xi \right) \times \left(\frac{T_u}{T_0}(\tau, 0) - \tilde{T}_w(\tau) \right) + \tilde{T}_w(\tau). \qquad \text{(A-13)}$$

This is the analytical expression of the transient mold wall temperature.

APPENDIX B. DYNAMIC MOLD WALL TEMPERATURE WITH NEWTONIAN CONVECTION BOUNDARY CONDITION

For polymer reaction molding with flow or continuous flow type chemical reactor, the local heat exchange between the reacting fluid and the wall is usually expressed by a Newtonian convection boundary condition.

$$-k_s \frac{\partial T_s}{\partial y} = h_u(\langle T_u \rangle - T_s) \quad \text{at } y = d \quad \text{for } t > 0 \qquad \text{(B-1)}$$

where h_u is the heat transfer coefficient on the wall and $\langle T_u \rangle$ is the cup mixing temperature or the average flow temperature of the fluid.

If we define

$$Bi' = \frac{h_u d_1}{k_s}, \quad \text{and} \quad \langle \theta_u \rangle = \frac{\langle T_u \rangle - T_w}{T_0},$$

the heat conduction equation (15) becomes

$$\frac{\partial \theta}{\partial \tau} = \frac{\partial^2 \theta}{\partial \xi^2}, \qquad \text{(B-2)}$$

with I.C.

$$\theta(0, \xi) = 0 \quad \text{for} \quad 0 \le \xi \le 1,$$

and B.Cs.

$$\frac{\partial \theta}{\partial \xi}(\tau, 0) + Bi'[\langle \theta_u(\tau) \rangle - \theta(\tau, 0)] = 0,$$

$$\frac{\partial \theta}{\partial \xi}(\tau, 1) + Bi\theta(\tau, 1) = 0.$$

The same technique used above can be applied here. We define

$$V(\tau, \xi) = \theta(\tau, \xi) + B(\xi) \langle \theta_u(\tau) \rangle, \qquad \text{(B-3)}$$

with

$$B(\xi) = \left(\frac{Bi}{1+Bi} \xi - 1 \right) \Big/ \left(1 + \frac{Bi}{(1+Bi)Bi'} \right),$$

and

$$\phi_n(\xi) = \frac{\lambda_n}{Bi'} \cos \lambda_n \xi + \sin \lambda_n \xi, \qquad \text{(B-4)}$$

where λ_n is the nth eigenvalue of the characteristic equation

$$\tan \lambda = \frac{(Bi + Bi')\lambda}{\lambda^2 - BiBi'}. \qquad \text{(B-5)}$$

The solution of mold (or reactor) wall temperature is

$$\tilde{T}_s(\tau, \xi) = \sum_{n=1}^{\infty} P'_n \left[\frac{T_{u0}}{T_0} \langle \tilde{T}_u(\tau) \rangle - \tilde{T}_w(\tau) - \lambda_n^2 \times e^{-\lambda_n^2 \tau} \int_0^\tau e^{\lambda_n^2 \tilde{\tau}} \left(\frac{T_{u0}}{T_0} \langle \tilde{T}_u(\tilde{\tau}) \rangle - \tilde{T}_w(\tilde{\tau}) \right) d\tilde{\tau} \right] \times \left(\sin \lambda_n \xi + \frac{\lambda_n}{Bi'} \cos \lambda_n \xi \right) - B(\xi) \times \left(\frac{T_{u0}}{T_0} \langle \tilde{T}_u(\tau) \rangle - \tilde{T}_w(\tau) \right) + \tilde{T}_w(\tau), \qquad \text{(B-6)}$$

where

$$P'_n = \left[\frac{p_1}{p_2} (\sin \lambda_n / \lambda_n^2 - \cos \lambda_n / \lambda_n) + (\cos \lambda_n - 1)/\lambda_n - \sin \lambda_n / Bi' + \frac{p_1 \lambda_n}{p_2 Bi'} \times (\cos \lambda_n / \lambda_n^2 + \sin \lambda_n / \lambda_n - 1/\lambda_n^2) \right] \Big/ [(\lambda_n - \sin \lambda_n \cos \lambda_n)/2\lambda_n + \sin^2 \lambda_n / Bi' + \lambda_n^2 (\sin \lambda_n \cos \lambda_n / \lambda_n + 1)/2Bi'^2],$$

and

$$p_1 = Bi/(1 + Bi), \qquad p_2 = 1 + \frac{Bi}{(1 + Bi)Bi'}.$$

From equation (B-6), it is easy to see that the no flow case, equation (24), is a special case of the general dynamic equation (B-6) in which $Bi' = \infty$.

TRANSFERT THERMIQUE LORS DU MOULAGE D'UN POLYMERE EN REACTION

Résumé—On propose un modèle théorique de la réaction de polymérisation lors du moulage avec une température du moule controlée par une circulation de fluide. On néglige la convection et la diffusion de masse. Une technique modifiée de séparation des variables pour la conduction thermique est utilisée afin de déterminer une expression analytique du profil non stationnaire de la température de la paroi du moule. Le résultat est ensuite combiné avec les équations aux dérivées partielles non linéaires des bilans de chaleur et de masse et traité numériquement. On considère aussi température quasi-statique de température de moule. Ce cas simplifie beaucoup les conditions aux limites. L'hypothèse du quasistatique est testée pour différents cas et on trouve qu'elle est applicable au moulage d'un polymère. Le nombre de Biot pour le transfert thermique peut être utilisé comme un paramètre adapté à la description de la condition limite à la surface du polymère.

Le modèle est testé avec la polymérisation rapide RIM du polyuréthane dans un moule plat équipé de thermocouples. Différents matériaux pour la paroi de moule sont utilisés. Les mesures de profils de température dans le polymère et à la paroi se comparent favorablement aux prévisions du modèle.

WÄRMEÜBERTRAGUNG BEI FORMGEBUNGSVERFAHREN VON REAGIERENDEN POLYMEREN

Zusammenfassung—Es wird ein theoretisches Modell vorgeschlagen für die Aushärtung von Polymeren bei Reaktions-Formgebungsverfahren wie Gießen, Formen von Thermoplasten oder Spritzformen, bei denen die Temperatur der Form durch Flüssigkeitsumlauf in der Formwand geregelt wird. Konvektion und Massediffusion werden vernachlässigt. Es wird eine abgewandelte Methode der Variablentrennung für das Wärmeleitproblem bei zeitabhängigen Randbedingungen benutzt, um einen analytischen Ausdruck für die instationäre Wandtemperatur der Gießform zu erhalten. Das Ergebnis wird dann mit den nichtlinearen Differentialgleichungen der Wärme- und Massenbilanz in vernetzenden Polymeren kombiniert und numerisch gelöst. Der Fall quasistationärer Formwandtemperaturen wird auch betrachtet. Hierbei vereinfachen sich die Randbedingungen erheblich. Die quasistationäre Annahme wird für verschiedene Fälle geprüft und gefunden, daß sie auf Formgebungsverfahren von Polymeren anwendbar ist. Die Wärmeübergangsrandbedingung läßt sich an der Polymeroberfläche gut durch die Biot-Zahl beschreiben. Das Modell wurde mit einem schnell polymerisierenden Spritzform-Polyurethan in einer Plattenform überprüft, welche mit Thermoelementen instrumentiert war. Es wurden verschiedene Gußformwandwerkstoffe verwendet. Messungen des Temperaturprofils in der Polymerplatte und der Gußformwand stimmen gut mit den Modellrechnungen überein.

ТЕПЛОПЕРЕНОС В ПРЕССФОРМЕ, ЗАПОЛНЕННОЙ ПОЛИМЕРИЗИРУЮЩИМСЯ ВЕЩЕСТВОМ

Аннотация — Предложена теоретическая модель отверждения при полимеризации в процессе разливки, термореактивной формовки и формовки под давлением, когда температура прессформы контролируется жидкостью, циркулирующей по ее стенкам. Конвекция и диффузия массы не учитываются. Нестационарный профиль температур стенок прессформы определяется модифицированным методом разделения переменных, применяемым в задачах теплопроводности при зависящих от времени граничных условиях. Полученные результаты вводятся в нелинейные дифференциальные уравнения баланса тепла и массы для процесса отверждения полимеров и дается численное решение. Также рассматривается случай квазистационарной температуры стенок прессформы, когда граничные условия значительно упрощены. Допущение о квазистационарности температуры проверено для нескольких случаев и показано, что оно является справедливым при формовке полимеризацией. Критерий Био может быть использован как удобный параметр для описания граничных условий на поверхности полимера. Справедливость модели проверена в случае формовки полимеризацией под давлением полиуретана в виде плиты, в которую заделывались термопары. Прессформа изготавливалась из различных материалов. Полученные распределения температуры в плите и прессформе хорошо согласуются с результатами расчетов в соответствии с предложенной моделью.